Inorg. Chem. **2003**, *42*, 7219–7226

Inorganic Chemistry
Article

Reactions of Palladium Germylene Complexes: Formation of Sulfide Bridges

Zuzanna T. Cygan, Jeff W. Kampf, and Mark M. Banaszak Holl*

Department of Chemistry, University of Michigan, Ann Arbor, Michigan 48109-1055

Received June 3, 2003

Reactivity of three novel Pd germylene species is presented. $(Et_3P)_2PdGe[N(SiMe_3)_2]_2$ (**1**) and $(dppe)PdGe[N(SiMe_3)_2]_2$ (**6**) react with COS to give the sulfide bridged species $(Et_3P)_2Pd(\mu S)Ge[N(SiMe_3)_2]_2$ (**2**) and $(dppe)Pd(\mu S)Ge[N(SiMe_3)_2]_2$ (**7**) (dppe = (diphenylphosphino)ethane). $(Ph_3P)_2PdGe[N(SiMe_3)_2]_2$ (**4**) reacts with COS to give the disulfide bridged complex $(Ph_3P)_2Pd(\mu S)_2Ge[N(SiMe_3)_2]_2$ (**5**) resulting in Pd–Ge bond cleavage. This phosphine dependent reactivity is explored. Crystal structures of **2**, **5**, **7**, and the dimeric form of complex **2**, $\{(Et_3P)Pd(\mu S)Ge[N(SiMe_3)_2]_2\}_2$ (**8**), are reported. In the presence of excess germylene, complexes **2** and **5** are shown to partially regenerate their parent palladium germylene complexes, **1** and **4**, respectively, via photolysis or heating.

Introduction

Germylenes are divalent germanium species, containing a singlet lone pair capable of interacting with metals in a dative bonding sense, as well as an empty π-acidic p orbital localized on the Ge^{II} center.[1−7] The close proximity of the electron rich metal and the Lewis acidic Ge^{II} suggests a variety of addition reactions should be possible across the metal−germylene bond. However, the majority of the chemistry of the M−Ge bond has been studied in the context of Ge^{IV} species: illustrative examples include germylation reactions utilizing a metal catalyst,[8−15] the metal catalyzed formation of Ge containing polymers,[16−18] or cross coupling reactions.[19]

Germanium has been explored as a promoter for palladium-based hydrogenation catalysts. A variety of interesting activity and selectivity enhancements have been observed for the hydrogenation of double bonds.[20] The electrocatalytic reduction of nitrate to hydroxylamine using germanium promoters on a palladium electrode is also quite effective.[21,22] In addition, germanium has been explored to develop sulfur-resistant hydrogenation catalyst systems.[23] The germanium

---

* To whom correspondence should be addressed. E-mail: mbanasza@umich.edu.

(1) Schriewer, M.; Neumann, W. P. *J. Am. Chem. Soc.* **1983**, *105*, 897−901.
(2) Barthelat, J. C.; Roch, B. S.; Trinquier, G.; Satgé, J. *J. Am. Chem. Soc.* **1980**, *102*, 4080−4086.
(3) Petz, W. *Chem. Rev.* **1986**, *86*, 1019−1047.
(4) Lappert, M. F.; Rowe, R. S. *Coord. Chem. Rev.* **1990**, *100*, 267−292.
(5) Bazinet, P.; Yap, G. P. A.; Richeson, D. S. *J. Am. Chem. Soc.* **2001**, *123*, 11162−11167.
(6) Knorr, M.; Hallauer, E.; Huch, V.; Veith, M.; Braunstein, P. *Organometallics* **1996**, *15*, 3868−3875.
(7) Neuman, W. P. *Chem. Rev.* **1991**, *91*, 311−334.
(8) Mitchell, T. N.; Schneider, U.; Frohling, B. *J. Organomet. Chem.* **1990**, *384*, C53−C56.
(9) Chatani, N.; Horiuchi, N.; Hanafusa, T. *J. Org. Chem.* **1990**, *55*, 3393−3395.
(10) Reddy, N. P.; Hayashi, T.; Tanaka, M. *Chem. Lett.* **1991**, 677−680.
(11) Ikenaga, K.; Matsumoto, S.; Kikukawa, K.; Matsuda, T. *Chem. Lett.* **1990**, 185−188.
(12) Hayashi, T.; Yamashita, H.; Sakakura, T.; Uchimaru, Y.; Tanaka, M. *Chem. Lett.* **1991**, 245−248.
(13) Furukawa, N.; Kourogi, N.; Seki, Y.; Kakiuchi, F.; Murai, S. *Organometallics* **1999**, *18*, 3764−3767.
(14) Mochida, K.; Wada, T.; Suzuki, K.; Hatanaka, W.; Nishiyama, Y.; Nanjo, M.; Sekine, A.; Ohashi, Y.; Sakamoto, M.; Yamamoto, A. *Bull. Chem. Soc. Jpn.* **2001**, *74*, 123−137.
(15) Tsumuraya, T.; Ando, W. *Organometallics* **1990**, *9*, 869−871.
(16) Gomez, F. J.; Wagener, K. B. *J. Organomet. Chem.* **1999**, *592*, 271−277.
(17) Katz, S. M.; Reichl, J. A.; Berry, D. H. *J. Am. Chem. Soc.* **1998**, *120*, 9844−9849.
(18) Kobayashi, S.; Iwata, S.; Abe, M.; Shoda, S. *J. Am. Chem. Soc.* **1990**, *112*, 1625−1626.
(19) David-Quillot, F.; Thibonnet, J.; Marsacq, D.; Abarbri, M.; Duchene, A. *Tetrahedron Lett.* **2000**, *41*, 9981−9984.
(20) Bodnar, Z.; Mallat, T.; Bakos, I.; Szabo, S.; Zsoldos, Z.; Schay, Z. *Appl. Catal., A* **1993**, *102*, 105−123.
(21) Gootzen, J. F. E.; Peeters, P.; Dukers, J. M. B.; Lefferts, L.; Visscher, W.; vanVeen, J. A. R. *J. Electroanal. Chem.* **1997**, *434*, 171−183.
(22) Gootzen, J. F. E.; Lefferts, L.; van Veen, J. A. R. *Appl. Catal., A* **1999**, *188*, 127−136.
(23) Guillon, E.; Lynch, J.; Uzio, D.; Didillon, B. *Catal. Today* **2001**, *65*, 201−208.

10.1021/ic034613z CCC: $25.00

promoter for all of these cases is typically GeO_2 or $GeCl_4$; however, spectroscopic studies indicate that these species are readily reduced by the palladium metal to be Ge(0) or Ge(II).[20,24,25] The majority species present is generally believed to be Ge(0);[25] however, the state of the catalytically active species has not been determined.

Despite a number of interesting catalysis studies, the role of the germanium promoter is largely unknown, and the chemical interactions of palladium, germanium, and sulfur are not understood. Unfortunately, the catalytic work does not have a substantial basis in solution phase chemistry to provide a basis for comparisons and guidance regarding anticipated structures or chemical conversions. Very little structural chemistry of the Pd/Ge system has been explored; just a handful of molecular species with $Ge^{(II)}$ have been characterized,[26−28] and no molecular species highlighting the interactions of sulfur with Pd/Ge systems have been synthesized.

In this report, we present an initial exploration of the chemistry of Pd/Ge complexes of the general formula $L_2PdGe[N(SiMe_3)_2]_2$ where L represents monodentate or bidentate phosphines. The reaction of COS displays a new mode of heterocumulene reactivity with the M−Ge bond vector, generating a class of molecules that highlight cooperative reactivity with S by both the Pd and Ge metal centers. We demonstrate the ability of the Ge(II) to sequester S and reduce the Pd metal, illustrating the potential of Ge(II) to reverse the effect of sulfur poisoning of Pd catalysts.

Experimental Section

All manipulations were performed using air-free techniques. Benzene, toluene, THF, and benzene-d_6 were dried over sodium benzophenone ketyl and degassed. Acetonitrile was dried over 4 Å molecular sieves and degassed. COS (Aldrich, Pfaltz and Bauer) was purchased commercially and used as received. $Ge[N(SiMe_3)_2]_2$,[29] $(Et_3P)_2PdGe[N(SiMe_3)_2]_2$ (**1**),[26] $(Ph_3P)_2PdGe[N(SiMe_3)_2]_2$ (**4**),[26] and $(dppe)PdGe[N(SiMe_3)_2]_2$ (**6**)[26] were prepared according to published procedures. ^1H, ^{31}P, and ^{13}C NMR spectra were acquired on a Varian 400 MHz instrument (400, 161.9, and 100.6 MHz, respectively) or on a Varian 300 MHz instrument (300 MHz ^1H, 121.5 MHz ^{31}P). ^{31}P NMR spectra are referenced to H_3PO_4 by using an external secondary standard of PPh_3 in benzene-d_6 (assigned to −5.0 ppm).[30] UV−vis spectra were acquired on a Shimadzu UV-1601.

$(Et_3P)_2\overline{Pd(\mu S)Ge}[N(SiMe_3)_2]_2$ (2). In a 250 mL round-bottom flask, **1** (800 mg, 0.1 mmol) was dissolved in 70 mL of toluene and cooled to 0 °C. To the orange solution, 1.4 equiv of COS was added by measured gas bulb addition. The solution was allowed to stir for 2 h at 0 °C and slowly changed color to a yellow brown, with the evolution of gas. The volatiles were evacuated leaving a brown solid. The crude product was recrystallized from THF/acetonitrile to give 589 mg (70% yield) of light yellow **2.** ^1H NMR (C_6D_6) δ 0.59 (s, 36H, $SiMe_3$), 0.90 (m, 18H, CH_3) 1.62 (m, 12H, CH_2). Note: The ethyl groups of the phosphine ligands display accidental overlap in their ^1H NMR resonances. ^{31}P NMR and ^{13}C NMR spectra indicate that the two phosphine ligands are chemically inequivalent. $^{31}P\{^1H\}$ NMR (C_6D_6) δ 6.11 (d, $^2J_{P-P}$ 42 Hz) 16.91 (d, $^2J_{P-P}$ 42 Hz). ^{13}C $\{^1H\}$ NMR δ 6.78 (s, $SiCH_3$), 8.23 (s, CH_2CH_3), 9.04 (s, CH_2CH_3), 16.53 (d, CH_2CH_3, J_{P-C} 14 Hz), 21.16 (d, CH_2CH_3, J_{P-C} 16 Hz). Calcd for $C_{24}H_{66}GeN_2P_2PdSSi_4$: C 37.52, H 8.66, N 3.65. Found: C 37.13, H 8.30, N 3.32. UV−vis (pentane) λ_{max} 356 nm (ϵ 12000 M^{-1} cm^{-1}), 262 nm (ϵ 20000 M^{-1} cm^{-1}), 242 nm (ϵ 21000 M^{-1} cm^{-1}).

$(Ph_3P)_2Pd(\mu S)_2Ge[N(SiMe_3)_2]_2$ (5). In a 100 mL round-bottom flask, **4** (150 mg, 0.14 mmol) was dissolved in 30 mL of toluene. To the orange solution, 4.4 equiv of COS was added. The solution gradually darkened to a brown color, and the evolution of gas was observed. The solution was allowed to stir for 5 h. The volatiles were evacuated leaving a yellow brown solid. The crude product was recrystallized from THF/acetonitrile giving 67 mg (67%) of a tan solid. ^1H NMR (C_6D_6) δ 0.68 (s, 36H, $SiMe_3$), 6.89 (m, 18H, Ph), 7.56 (m, 12H, Ph). $^{31}P\{^1H\}$ NMR (C_6D_6) δ 31.28 (s). ^{13}C $\{^1H\}$ NMR δ 7.01 (s, $SiCH_3$), 127.88 (s, Ph), 127.96 (s, Ph), 130.11 (s. Ph), 135.25 (s, Ph). Calcd for $C_{48}H_{66}GeN_2P_2PdS2Si_4$: C 52.96, H 6.11, N 2.57. Found: C 52.77, H 5.89, N 2.27. UV−vis (THF) λ_{max} 350 nm (ϵ 11000 M^{-1} cm^{-1}), 295 nm (ϵ 26000 M^{-1} cm^{-1}).

$(dppe)\overline{Pd(\mu S)Ge}[N(SiMe_3)_2]_2$ (7). A 100 mL round-bottom flask was charged with 150 mg of **6** (0.17 mmol). Toluene (5 mL) was distilled into the flask forming an orange solution. COS (3.2 equiv) was added and the solution stirred at room temperature. The solution was observed to liberate gas and slowly darkened to a brown color. After 40 h of stirring, the volatiles were stripped leaving a light brown solid. Crystals were grown by slow evaporation of THF and were removed from the mother liquor giving 61 mg (37%) of analytically pure **7**. ^1H NMR (C_6D_6) δ 0.50 (s, 36H, $SiMe_3$), 1.69 (m, 1H, CH_2), 1.74 (m, 1H, CH_2), 1.95 (m, 1H, CH_2), 2.02 (m, 1H,CH_2), 6.98 (m, 2H, Ph) 7.03 (m, 10H, Ph), 7.51 (m, 4H, Ph), 7.95 (m, 4H, Ph). ^1H NMR (THF-d_8) δ 0.18 (s, 36H, $SiMe_3$), 2.19 (m, 1H, CH_2), 2.24 (m, 1H, CH_2), 2.47 (m, 1H, CH_2), 2.54 (m, 1H,CH_2), 7.36 (m, 10H, Ph), 7.39 (m, 2H, Ph), 7.63 (m, 4H, Ph), 8.01 (m, 4H, Ph). $^{31}P\{^1H\}$ NMR (C_6D_6) δ 28.9 (d, J_{P-P} 33 Hz), 44.16 (d, J_{P-P} 33 Hz). $^{31}P\{^1H\}$ NMR (THF-d_8) δ 34.1 (d, J_{P-P} 35 Hz), 48.63 (d, J_{P-P} 35 Hz). ^{13}C NMR (THF-d_8) δ 6.53 (s, $SiMe_3$), 23.04 (d, CH_2 J_{P-C} 22 Hz), 25.54 (d, CH_2 J_{P-C} 21 Hz), 129.27 (d, Ph J_{P-C} 3 Hz), 129.37 (d, Ph J_{P-C} 2 Hz), 130.86 (d, Ph J_{P-C} 2 Hz), 131.22 (d, Ph J_{P-C} 2 Hz), 134.02, 134.15, 134.42, 134.55, 134.65, 134.82, 134.91, 135.18 (s, Ph). EA was obtained on crystals grown from THF solution. Calcd for $C_{38}H_{60}GeN_2O_2P_2PdSSi_4{\cdot}C_4H_8O$: C 50.32, H 6.84, N 2.79. Found: C 50.36, H 6.79, N 2.74.

$\{(Et_3P)\overline{Pd(\mu S)Ge}[N(SiMe_3)_2]_2\}_2$ (8). In a 250 mL round-bottom flask, **1** (1 g, 1.35 mmol) was dissolved in ∼50 mL of toluene. To the orange solution, 1.1 equiv of COS was added by measured gas bulb addition. The solution quickly changed color to a light brown, and the evolution of gas was observed. The solution was allowed to stir for 46 h. The volatiles were evacuated leaving a brown solid. A 200 mg portion of this solid was recrystallized from THF/acetonitrile giving a brown solid. This solid was then recrystallized from pentane giving a brown solid and darker brown filtrate. The volatiles were evaporated from the filtrate giving a dark brown residue. Benzene-d_6 (ca 0.5 mL) was used to rinse out a small

---

[24] Bodnar, Z.; Mallat, T.; Baiker, A. *J. Electroanal. Chem.* **1993**, *358*, 327−331.

[25] Pijpers, A. P.; Lefferts, L. *Appl. Catal., A* **1999**, *185*, 29−39.

[26] Cygan, Z. T.; Bender, J. E.; Litz, K. E.; Banaszak Holl, M. M. *Organometallics* **2002**, *21*, 5373−5381.

[27] Hitchock, P. B.; Lappert, M. F.; Misra, M. C. *J. Chem. Soc., Chem. Commun.* **1985**, 863−865.

[28] Campbell, G. K.; Hitchcock, P. B.; Lappert, M. F.; Misra, M. C. *J. Organomet. Chem.* **1985**, *289*, C1−C4.

[29] Gynane, M. J. S.; Harris, D. H.; Lappert, M. F.; Power, P. P.; Riviere, P.; Riviere-Baudet, M. *J. Chem. Soc., Dalton Trans.* **1977**, 2004−2009.

[30] Lawson, H. J.; Atwood, J. D. *J. Am. Chem. Soc.* **1989**, *111*, 6223−6227.

Table 1. Summary of Crystallographic Data for **2**, **5**, **7**, and **8**

	2	**5**	**7·THF**	**8·C_6D_6**
empirical formula	$C_{24}H_{66}GeN_2P_2PdSSi_4$	$C_{54}H_{72}GeN_2P_2PdS_2\ Si_4$	$C_{42}H_{68}GeN_2OP_2PdSSi_4$	$C_{42}H_{108}Ge_2N_4P_2Pd_2S_2Si_8$
fw	768.14	1166.55	1002.33	1378.08
temp	158(2) K	158(2) K	158(2) K	158(2) K
cryst syst, space group	monoclinic, $P2_1/n$	orthorhombic, $P2_12_12_1$	monoclinic, $C2/c$	triclinic, $P\bar{1}$
unit cell dimensions	$a = 16.064(3)$ Å $b = 13.205(2)$ Å $c = 36.708(7)$ Å $\alpha = 90°$ β=90.346(3)° $\gamma = 90°$	$a = 13.0526(14)$ Å $b = 20.666(2)$ Å $c = 22.719(2)$ Å $\alpha = 90°$ $\beta = 90°$ $\gamma = 90°$	$a = 38.3831(19)$ Å $b = 12.1176(5)$Å $c = 22.3611(11)$ Å $\alpha = 90°$ β=106.421(2)° $\gamma = 90°$	$a = 11.2870(13)$ Å $b = 12.7506(15)$Å $c = 13.1569(15)$Å $\alpha = 105.478(2)°$ $\beta = 112.702(2)°$ $\gamma = 90.475(2)°$
V	7787(2) A^3	6128.5(11) Å^3	9976.2(8) Å^3	1670.2(3) Å^3
Z, calcd d	8, 1.310 Mg/m^3	4, 1.264 Mg/m^3	8, 1.335 Mg/m^3	1, 1.370 Mg/m^3
abs coeff	1.509 mm^{-1}	1.016 mm^{-1}	1.197 mm^{-1}	1.705 mm^{-1}
λ	0.71073 Å	0.71073 Å	0.71073 Å	0.71073 Å
final R indices [$I > 2\sigma(I)$]	R1 = 0.0392, $wR^2 = 0.0769$	R1 = 0.0352, $wR^2 = 0.0770$	R1 = 0.0229, $wR^2 = 0.0568$	R1 = 0.0214, $wR^2 = 0.0544$
R indices (all data)	R1 = 0.0486, $wR^2 = 0.0813$	R1 = 0.0432, $wR^2 = 0.0799$	R1 = 0.0279, $wR^2 = 0.0588$	R1 = 0.0253, $wR^2 = 0.0566$

amount of the residue for NMR, and the remaining drops of benzene were left in the flask to evaporate. Several red crystals of **8** were collected after 3 days. ^1H NMR (C_6D_6) δ 0.60 (s, 36H, $SiMe_3$), 1.2 (m, 9H, CH_3) 1.77 (m, 6H, CH_2). $^{31}P\{^1H\}$ NMR (C_6D_6) δ 18.2 (s).

Structure Determination of 2. Yellow blocks of **2** were crystallized from tetrahydrofuran at room temperature. A crystal of dimensions 0.36 × 0.36 × 0.30 mm^3 was mounted on a standard Bruker SMART CCD-based X-ray diffractometer equipped with a LT-2 low temperature device and normal focus Mo-target X-ray tube ($\lambda = 0.71073$ Å) operated at 2000 W power (50 kV, 40 mA). The X-ray intensities were measured at 158(2) K; the detector was placed at a distance 4.959 cm from the crystal. A total of 2490 frames were collected with a scan width of 0.3° in ω and φ with an exposure time of 30 s/frame. The frames were integrated with the Bruker SAINT software package[31] with a narrow frame algorithm. The integration of the data yielded a total of 86356 reflections to a maximum 2θ value of 56.62° of which 19850 were independent and 16563 were greater that 2$\sigma(I)$. The θ range for data collection was 2.07−28.36°. The final cell constants (Table 1) were based on the *xyz* centroids of 7178 reflections above 10$\sigma(I)$. Analysis of the data showed negligible decay during data collection; the data were processed with SADABS[32] and corrected for absorption. The crystals form as pseudo-orthorhombic merohedral twins (twin law 1 0 0, 0 −1 0, 0 0 −1, twin fraction 0.0727(5)) and two crystallographically independent molecules in the asymmetric unit. The structure was solved and refined with the Bruker SHELXTL software package,[33] using the space group $P2_1/n$ with $Z = 8$ for the formula $C_{24}H_{66}N_2P_2Si_4SGePd$. All non-hydrogen atoms were refined anisotropically with the hydrogen atoms placed in idealized positions. The ethyl carbons of one triethylphosphine ligand (P1) are rotationally disordered over two closely related positions. Partial occupancy atoms and modest restraints allowed for a chemically sensible modeling of the disorder. Limiting indices: $-21 \le h \le 21$, $-17 \le k \le 17$, $-48 \le l \le 48$. See Table 1 for additional details.

Structure Determination of 5. Yellow plates of **5** were grown from a benzene-d_6 solution at room temperature. A crystal of dimensions 0.26 × 0.26 × 0.16 mm^3 was mounted as for **2**. The X-ray intensities were measured at 158(2) K; the detector was placed at a distance 4.959 cm from the crystal. A total of 2018 frames were collected with a scan width of 0.3° in ω and φ with an exposure time of 30 s/frame. The frames were integrated with the Bruker SAINT software package[31] with a narrow frame algorithm. The integration of the data yielded a total of 53009 reflections to a maximum 2θ value of 52.85° of which 12558 were independent and 11204 were greater than 2$\sigma(I)$. The θ range for data collection was 3.26−26.41°. The final cell constants (Table 1) were based on the *xyz* centroids of 6734 reflections above 10$\sigma(I)$. Analysis of the data showed negligible decay during data collection; the data were processed with SADABS[32] and corrected for absorption. The structure was solved and refined with the Bruker SHELXT software package,[33] using the space group $P2_12_12_1$ with $Z = 4$ for the formula $C_{54}H_{72}N_2S_2Si_4P_2GePd$ which includes the contribution of a benzene lattice solvate molecule. All non-hydrogen atoms were refined anisotropically with the hydrogens placed in idealized positions. Limiting indices: $-16 \le h \le 16$, $-25 \le k \le 25$, $-28 \le l \le 28$. See Table 1 for additional details.

Structure Determination of 7. Yellow plates of **7** were crystallized from a THF/benzene solution at room temperature. A crystal of dimensions 0.58 × 0.44 × 0.40 mm^3 was cut from a larger plate and mounted as for **2**. The X-ray intensities were measured at 158(2) K; the detector was placed at a distance 4.959 cm from the crystal. A total of 2937 frames were collected with a scan width of 0.3° in ω and φ with an exposure time of 20 s/frame. The frames were integrated with the Bruker SAINT software package[31] with a narrow frame algorithm. The integration of the data yielded a total of 126271 reflections to a maximum 2θ value of 56.71° of which 12918 were independent and 10918 were greater than 2$\sigma(I)$. The final cell constants (Table 1) were based on the *xyz* centroids of 6751 reflections above 10$\sigma(I)$. The θ range for data collection was 3.30−28.30°. Analysis of the data showed negligible decay during data collection; the data were processed with SADABS[32] and corrected for absorption. The structure was solved and refined with the Bruker SHELXTL software package,[33] using the space group $C2/c$ with $Z = 8$ for the formula $C_{38}H_{60}N_2P_2SSi_4PdGe\cdot(THF)$. All non-hydrogen atoms were refined anisotropically with the hydrogen placed in idealized positions. Limiting indices: $-51 \le h \le 49$, $-16 \le k \le 16$, $-29 \le l \le 29$. The THF lattice solvate is disordered over two orientations. See Table 1 for additional details.

Crystal Structure Determination of 8. Orange blocks of **8** were crystallized from a benzene-d_6 solution at room temperature. A crystal of dimensions 0.60 × 0.48 × 0.32 mm^3 was mounted as

---

(31) *Saint Plus, v. 6.02*; Bruker Analytical X-ray: Madison, WI, 1999.

(32) Sheldrick, G. M. *SADABS. Program for Empirical Absorption Correction of Area Detector Data*; University of Göttingen: Göttingen, Germany, 1996.

(33) Sheldrick, G. M. *SHELXTL, v. 5.10*; Bruker Analytical X-ray: Madison, WI, 1997.

for **2**. The X-ray intensities were measured at 158(2) K; the detector was placed at a distance of 4.939 cm from the crystal. A total of 3008 frames were collected with a scan width of 0.3° in ω and φ with an exposure time of 10 s/frame. The frames were integrated with the Bruker SAINT software package[31] with a narrow frame algorithm. The integration of the data yielded a total of 21115 reflections to a maximum 2θ value of 56.65° of which 8130 were unique and 7375 were greater than $2\sigma(I)$. The final cell constants (Table 1) were based on the *xyz* centroids of 7856 reflections above $10\sigma(I)$. The θ range for data collection was 3.42−28.32°. Analysis of the data showed negligible decay during data collection; the data were processed with SADABS[32] and corrected for absorption. The structure was solved and refined with the Bruker SHELXTL software package,[33] using the space group $P\bar{1}$ with $Z = 1$ for the formula $C_{36}H_{102}N_4P_2S_2Si_8Ge_2Pd_2 \cdot (C_6D_6)$. The Pd−Ge complex and the benzene solvate are both located on inversion centers in the crystal lattice. All non-hydrogen atoms were refined anisotropically with the hydrogen atoms located on a difference Fourier map and allowed to refine isotropically. Limiting indices: $-15 \leq h \leq 13$, $-16 \leq k \leq 16$, $-17 \leq l \leq 17$. Additional details are presented in Table 1.

Reaction of 2 and 5 with Excess Germylene. NMR tubes fitted with Teflon valves were used. Each tube was filled with a benzene-d_6 solution containing 15 mg (0.02 mmol) of **2** and 38 mg (0.10 mmol) of Ge[N(SiMe$_3$)$_2$]$_2$, or 10 mg (0.009 mmol) of **5** and 18 mg (0.046 mmol) of Ge[N(SiMe$_3$)$_2$]$_2$. For photolysis experiments, the tubes were placed in a water bath beneath a Blak-Ray long wave (365 nm) ultraviolet lamp. For heating experiments, the NMR tubes were first degassed by freezing and opening to vacuum, and then placed in an oil bath maintained at 63 ± 4 °C. A set of NMR tubes was also left out on the benchtop in ambient light at room temperature for comparison to photolyzed and heated samples. ^{1}H NMR, ^{31}P NMR, and ^{13}C NMR spectra were acquired periodically to monitor reaction progress. Percentages of conversion were calculated by comparing integrations of resonances in the ^{31}P NMR spectra. Control reactions were carried out with NMR tubes containing solutions of **1** or **4** without added germylene which were heated, photolyzed, or left out on the bench alongside the other experiments. Control reactions containing excess phosphine were run under the same conditions as already described with solutions containing 12 mg (0.015 mmol) of **2** and 11 μL (0.078 mmol) of PEt$_3$ or 9 mg (0.008 mmol) of **5** and 11 mg (0.04 mmol) of PPh$_3$.

Results and Discussion

Formation of μ-S Complexes. Addition of 1.6 equiv of COS to a room temperature toluene solution of (Et$_3$P)$_2$PdGe[N(SiMe$_3$)$_2$]$_2$ (**1**) results in the rapid darkening of the orange solution to a brown color with the evolution of a gas, presumably CO. The resulting metal complex, (Et$_3$P)$_2$Pd(μ-S)Ge[N(SiMe$_3$)$_2$]$_2$ (**2**), contains a S atom bridging the Pd center and Ge center (see eq 1). The sulfide bridge is formed without cleavage of the Pd−Ge bond. The ^{31}P NMR spectrum of **2** reveals unsymmetrical phosphine ligands appearing as a pair of doublets at 6.11 and 16.91 ppm. In the ^{1}H NMR spectrum, the trimethylsilyl protons of the germylene ligand appear at 0.59 ppm, downshifted approximately 0.1 ppm from the starting material resonance.

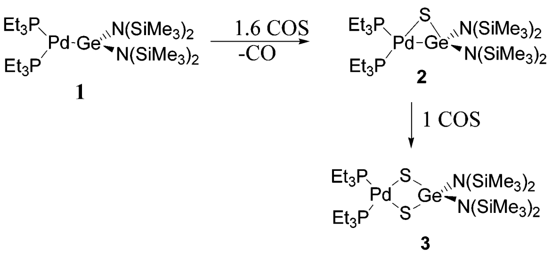

(1)

A change in the phosphine ligands of the parent palladium germylene complex has a pronounced effect on the reactivity with COS. The reaction of excess COS with (Ph$_3$P)$_2$PdGe[N(SiMe$_3$)$_2$]$_2$ (**4**) resulted in the formation of only one product: (Ph$_3$P)$_2$Pd(μS)$_2$Ge[N(SiMe$_3$)$_2$]$_2$ (**5**), a disulfide bridged species with a cleaved Pd−Ge bond (see eq 2). The

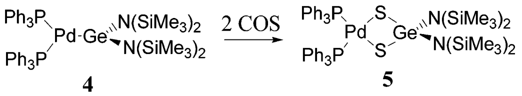

(2)

symmetric phosphines appear as a singlet at 31.28 ppm in the ^{31}P NMR. The trimethylsilyl protons of the germylene appear at 0.68 ppm in the ^{1}H NMR, a shift of 0.2 ppm downfield from the starting material.

We have also synthesized a palladium germylene complex that contains a bidentate ligand. (Dppe)PdGe[N(SiMe$_3$)$_2$]$_2$ exists in equilibrium in solution between its dimeric (**6a**) and monomeric (**6b**) forms (eq 3).[26] The addition of 3 equiv of COS to a ~1:1 mixture of **6a** and **6b** resulted in the formation of only one product, (dppe)Pd(μ-S)Ge[N(SiMe$_3$)$_2$]$_2$ (**7**). The ^{31}P NMR spectrum contains a pair of doublets at 44.16 and 28.8 ppm, and the trimethylsilyl resonance appears at 0.5 ppm in the ^{1}H NMR. There is no spectroscopic evidence for the formation of products with the dimeric form of the starting material, **6a**. This reactivity out of the monomeric form is similar to previously reported behavior of these complexes with O$_2$.[26]

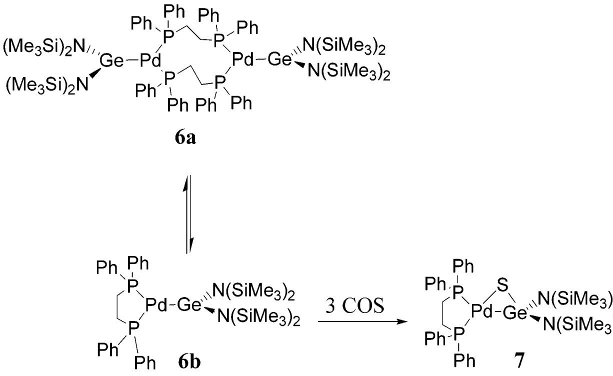

(3)

In order to further investigate the differing reactivity of **1** and **4** with COS, an isolated sample of **2** was allowed to react with one more equivalent of COS (eq 1). ^{1}H NMR and ^{31}P NMR spectra are consistent with the formation of the doubly bridged species (Et$_3$P)$_2$Pd(μS)$_2$Ge[N(SiMe$_3$)$_2$]$_2$ (**3**). A large singlet is present in the trimethylsilyl region at 0.75 ppm. Additionally, a singlet at 18.4 ppm in the ^{31}P NMR is consistent with equivalent phosphines. Although all of the starting material is consumed, **3** only represents 45% of the products formed as indicated by trimethylsilyl peaks in the ^{1}H NMR spectrum.

The formation of the first sulfide bridge to form **2** occurs within 15 min for 30 mM solutions of **1** in room temperature C_6D_6 in the presence of 1.1 equiv of COS. During this time period, conversion to disulfide-bridged **3** remains under 5% of the products formed. Formation of the second sulfide bridge to give **3** requires several hours and is not quantitative in contrast to the high yield reaction observed to form **5** (>90% ^{1}H NMR yield).

Complex **2** can be synthesized without the formation of complex **3** if the reaction is performed at low temperatures. A toluene solution of **2** was cooled to 0 °C, and 1.1 equiv of COS was added. After stirring for 2 h at 0 °C, the volatiles were stripped, and NMR spectra revealed the formation of **2**, without the formation of **3**. For comparison, room temperature experiments with 1.1−1.6 equiv of COS generated ~5% **3** over a 2 h period.

In order to compare to the conversion of **1** to **2**, $(Ph_3P)_2PdGe[N(SiMe_3)_2]_2$ (**4**) was allowed to react with 1 equiv of COS for approximately 4 h (eq 4). Although all the starting material was consumed, the only identifiable product was doubly bridged species **5** which formed in 20% yield. Several other unidentified products are also formed in this reaction although none had resonances assignable to a monobridged structure analogous to **2**. Most notably, there were no pairs of doublets in the ^{31}P NMR as expected for the two inequivalent phosphines present in a singly bridged species.

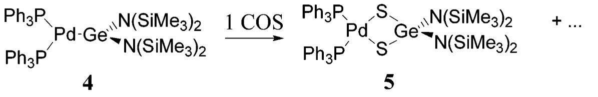

(4)

This difference in reactivity between complexes **1** and **4** can be rationalized in terms of the steric constraints of the phosphine ligands. PPh_3 is the largest of the three ligands, with a cone angle of 145° compared to 132° for PEt_3, and 125° for dppe.[34] A space filling model of **5** indicates that the second sulfide relieves steric interaction between the phosphine aryl groups and the germylene trimethylsilyl groups. A single sulfide bridge may result in greater steric crowding leading to enhanced lability of one of the PPh_3 ligands. The open site would provide an opportunity for reaction with the second equivalent of COS.

Common COS reactivity modes with transition metal complexes include σ complexes, π complexes, bridging of two metal centers, and insertion into various metal−heteroatom bonds.[35,36] If fragmentation of the COS molecule occurs, it usually acts as a carbonylation agent to deliver a CO ligand to the metal center. The S fragment can then react with another part of the metal complex, often a phosphine ligand, leaving as the phosphine sulfide. The formation of a sulfide complex and loss of CO is much rarer. Such a reaction was observed with $[(C_5H_4Me)_3U]\cdot THF$, which formed $[(C_5H_4Me)_3U]_2(\mu\text{-}S)$.[37] Reactions of Pd complexes with COS have yielded the addition of both a S and a CO fragment to the Pd metal centers[38] and the insertion of COS into two of the Pd ligand bonds.[39] The formation of $[PdS(COS)]_2$ from the reaction of COS with $PdCl_2$ has been proposed on the basis of IR assignments.[40] It is interesting that, in the presence of phosphine ligands, the reaction of COS with the palladium germylene complexes does not proceed via the carbonylation route. It is likely that the loss of CO drives this reaction, as attempts to make similar products from **1** using other sulfur sources such as S_8, CS_2, and ethylene sulfide were unsuccessful.

Previous work in our group with the Pt analogue of **1**, $(Et_3P)_2PtGe[N(SiMe_3)_2]_2$, demonstrated the cooperative reactivity of the transition metal and Ge center. Small molecules such as CO_2,[41] O_2,[42] and arylnitroso compounds[43] add across the Pt−Ge bond to form metallocyclic structures. In all cases, the Pt−Ge bond is preserved. The bridging molecule remains intact, and it simply adds the site of unsaturation to the Pt and Ge centers to make a four-membered ring. The complexes reported here differ in terms of the fragmentation of the substrate molecule, the size of the resulting metallocycle, and in the case of **5**, the cleavage of the M−Ge bond.

Complexes **2** and **7** also provide rare examples of a three-membered ring formed by the M−Ge bond and another atom. This structural motif is unprecedented in transition metal germylene complexes; however, there has been one report[4] of an unusually close interaction between a germylene and a chloride ligand in *cis*-$[RhCl(Ge[N(SiMe_3)_2]_2)(PPh_3)_2]$. The Ge···Cl distance was found to be 2.723(4) Å in the crystal structure of this complex.

An alternative bonding model for complexes **2** and **7** would be that of a germanethione bound to Pd via π donation, as shown in eq 5. Very few $R_2Ge{=}S$ species are known in the literature. Only four such species have been isolated, three stabilized by intramolecular coordination.[44] Only Tbt(Tip)Ge═S (Tbt = 2,4,6-tris[bis(trimethylsilyl)methyl]phenyl, Tip = 2,4,6-triisopropylphenyl) is kinetically stable.[45] Typical Ge−S single bond lengths range from 2.21 to 2.29 Å,[46] whereas the Ge═S bond length of Tbt(Tip)Ge═S is 2.049(3) Å,[45] and the calculated value for

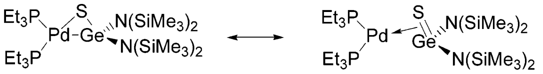

(5)

---

[34] Tolman, C. A. *Chem. Rev.* **1977**, *77*, 313−348.

[35] Pandey, K. K. *Coord. Chem. Rev.* **1995**, *140*, 37−114.

[36] Pandey, K. K.; Nigam, H. L. *Rev. Inorg. Chem.* **1984**, *6*, 69−94.

[37] Brennan, J. G.; Andersen, R. A.; Zalkin, A. *Inorg. Chem.* **1986**, *25*, 1761−1765.

[38] Tarlton, S. V.; Choi, N.; McPartlin, M.; Mingos, D. M. P.; Vilar, R. *J. Chem. Soc., Dalton Trans.* **1999**, 653−654.

[39] Werner, H.; Bertleff, W.; Schubert, U. *Inorg. Chim. Acta* **1980**, *43*, 199−204.

[40] Datta, S.; Agarwala, U. C. *Indian J. Chem., Sect. A: Inorg., Phys., Theor. Anal.* **1981**, *20*, 1190−1195.

[41] Litz, K. E.; Henderson, K.; Gourley, R. W.; Banaszak Holl, M. M. *Organometallics* **1995**, *14*, 5008−5010.

[42] Litz, K. E.; Banaszak Holl, M. M.; Kampf, J. W.; Carpenter, G. B. *Inorg. Chem.* **1998**, *37*, 6461−6469.

[43] Litz, K. E.; Kampf, J. W.; Banaszak Holl, M. M. *J. Am. Chem. Soc.* **1998**, *120*, 7484−7492.

[44] Lin, C. L.; Su, M. D.; Chu, S. Y. *Chem. Phys. Lett.* **2001**, *339*, 147−153.

[45] Matsumoto, T.; Tokitoh, N.; Okazaki, R. *J. Am. Chem. Soc.* **1999**, *121*, 8811−8824.

[46] Baines, K. M.; Stibbs, W. G. *Coord. Chem. Rev.* **1995**, *145*, 157−200.

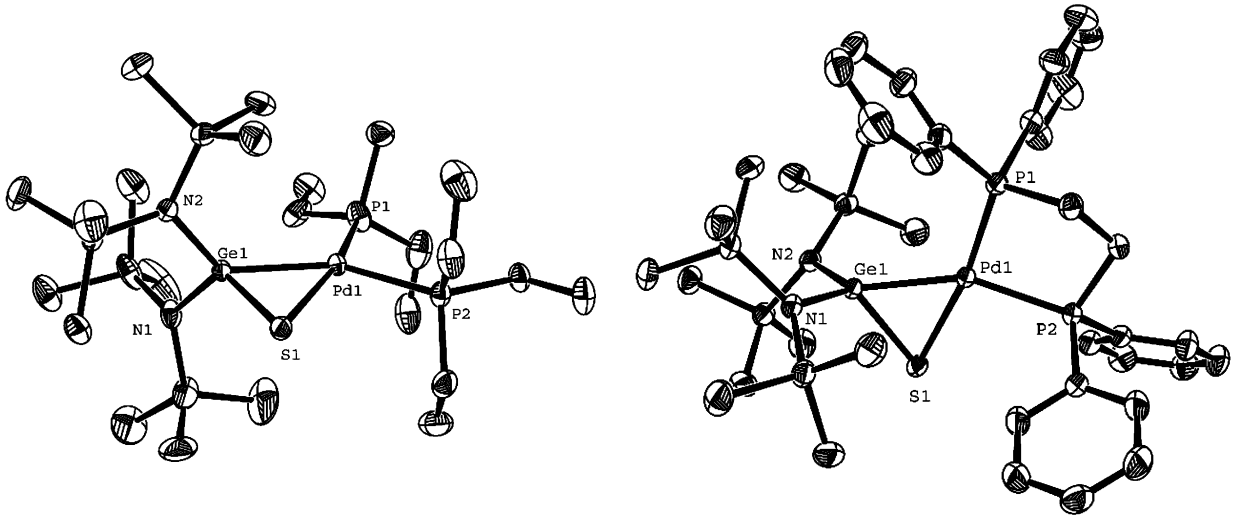

Figure 1. ORTEP representation (50% probability) of $(Et_3P)_2\overline{Pd(\mu S)Ge}[N(SiMe_3)_2]_2$ (**2**) and $(dppe)\overline{Pd(\mu S)Ge}[N(SiMe_3)_2]_2$ (**7**).

Table 2. Selected Bond Lengths (Å) and Angles (deg)

		2	
Pd−Ge 2.4092(5)	Pd−S 2.3769(10)	P−Pd−P 105.95(4)	S−Pd−Ge 54.27(2)
Pd_1-P_1 2.2911(11)	Ge−S 2.1830(1)	$Pd-Ge-N_2$ 125.69(9)	Ge−S−Pd 63.62(3)
Ge_1-N_1 1.875(3)	N−Ge−N 107.64(13)	$P_2-Pd-Ge$ 143.78(3)	S−Ge−Pd 62.11(3)
		5	
Pd_1-P_1 2.3213(10)	Ge_1-N_1 1.862(3)	$P_1-Pd_1-P_2$ 98.91(3)	$S_1-Pd_1-S_2$ 87.19(3)
Pd_1-S_1 2.3453(10)	Ge_1-S_1 2.1925(10)	$N_1-Ge_1-N_2$ 111.64(15)	$S_1-Ge_1-S_2$ 95.26(4)
$Pd_1\cdots Ge_1$ 3.17	$S_1-Ge_1-N_2$ 113.74(13)	$P_1-Pd_1-S_1$ 171.44(3)	$Pd-S_1-S_2-Ge$ 171.04(2)
		7	
Pd−Ge 2.4043(2)	Pd−S 2.3685(4)	N−Ge−N 108.75(6)	S−Ge−Pd 61.732(12)
Pd_1-P_1 2.2648(4)	Ge−S 2.1996(4)	Ge−S−Pd 63.390(11)	S−Pd−Ge 54.878(10)
Ge_1-N_1 1.8701(13)	P−Pd−P 85.887(14)	$P_2-Pd-Ge$ 155.312(12)	$Pd-Ge-N_2$ 128.32(4)
		8	
Pd_1-S_1 2.5055(5)	S_1-Ge_1 2.2169(5)	$P_1-Pd_1-Ge_{1A}$ 107.971(14)	$S_1-Pd_1-S_{1A}$ 107.304(14)
Pd_1-P_1 2.2674(4)	Pd_1-S_{1A} 2.4645(4)	$N_1-Ge_1-N_2$ 111.00(6)	$Pd_{1A}-S_1-Ge_1$ 59.951(11)
Ge_1-N_1 1.8621(13)	Pd_1-Ge_{1A} 2.3488(3)	$Ge_{1A}-Pd_1-S_{1A}$ 54.784(12)	$Pd_{1A}-Ge_1-S_1$ 65.256(12)
$S_{1A}-Pd_1-Pd_{1A}-S_1$ 180.00(2)	$Pd_1-S_1-S_{1A}-Pd_{1A}$ 180.00(2)	$Ge_{1A}-S_{1A}-Pd_1-S_1$ 179.9(3)	$Ge_1-Pd_{1A}-S_1-Pd_1$ 179.9(3)

$H_2Ge{=}S$ is 2.042 Å.[45] The Ge−S lengths of **2** and **7** are 2.1830(1) and 2.1996(4) Å, respectively. While this is slightly shorter than many previously reported values for Ge−S single bonds, there appears to be very little double bond character present. The Pd−S bond lengths of 2.3769(10) and 2.3685(4) Å also fall in the range of Pd−S single bonds that have been crystallographically characterized. A search of the Cambridge Structural Database System returned 1003 Pd−S single bonds averaging 2.32 ± 0.06 Å. Thus, σ donation through the S atom is the better bonding model for this interaction.

There is also no evidence for the formation of $[(Me_3Si)_2N]_2Ge{=}S$ free in solution. The reaction of $Ge[N(SiMe_3)_2]_2$ with elemental S results in a four-membered ring $\{[(Me_3Si)_2N]_2GeS\}_2$.[47] Such a structure would be essentially the dimeric structure of $[(Me_3Si)_2N]_2Ge{=}S$. No such products are observed in the ^1H NMR or ^{13}C NMR spectra of the reactions with COS.

Crystal Structures. The crystal structures of **2** and **7** are shown in Figure 1. In both structures, the constraint on the preferred geometry of the metal centers imparted by the sulfur bridge and Pd−Ge bond is clearly evident. The Pd^{II} metal centers takes on a distorted square planar geometry with a S−Pd−Ge angles of approximately 54°, and $P_2-Pd-Ge$ angles of 143.78(3)° and 155.312(12)° (see Table 2 for selected bond lengths and angles). The Ge centers are also distorted substantially from their preferred tetrahedral geometry with S−Ge−Pd angles of 62° and $Pd-Ge-N_2$ angles of 125.69(9)° and 128.32(4)°. In both structures, the Pd−Ge bond length is approximately 0.07 Å longer than that of the original palladium germylene complex.[26]

Unlike structures **2** and **7**, the ORTEP of **5** (Figure 2) shows a much less strained geometry about both the Pd and Ge metal centers. The Pd−Ge bond has been completely severed with a Pd⋯Ge distance of greater than 3.1 Å. This allows the Pd center to adopt a nearly square planar conformation. The $S_1-Pd_1-S_2$ angle is 87.19(3)°, and the $P_1-Pd_1-S_1$ angle is 171.44(3)°. The environment about the Ge center is also more tetrahedral than that in the other two structures, with $S_1-Ge_1-S_2$ and $S_1-Ge_1-N_2$ angles of 95.26(4)° and 113.74(13)°, respectively.

The $Pd_1-S_1-S_2-Ge_1$ dihedral angle of **5** is 171.04(2)°, indicating a slight hinging of the $\{M_2S_2\}$core on the S⋯S axis. Similar puckering has been found in X-ray diffraction

---

(47) Wegner, G. L.; Jockisch, A.; Schier, A.; Schmidbaur, H. *Z. Naturforsch.* **2000**, *55*, 347−351.

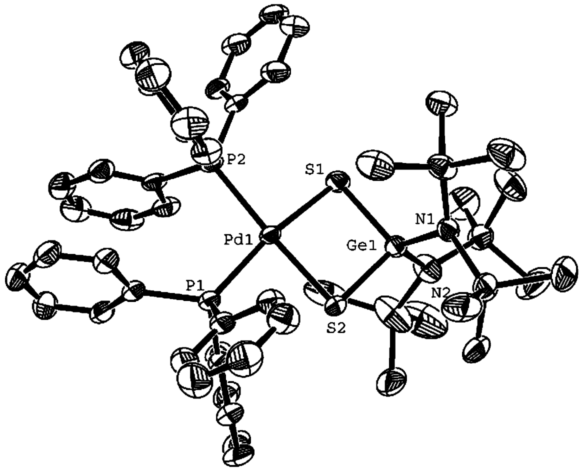

Figure 2. ORTEP representation (50% probability) of $(Ph_3P)_2Pd(\mu S)_2Ge[N(SiMe_3)_2]_2$ (**5**).

studies and ab initio calculations of complexes containing the $\{Pt_2S_2\}$core where terminal ligands on the Pt are small enough. Thus, Pt−S−S−Pt dihedral angles of 121° and 140° were found for $[Pt_2(PMe_2Ph)_4(\mu\text{-}S)_2]$[48] and $[Pt_2(dppe)_2(\mu\text{-}S)_2]$[49], respectively, and calculated to be as low as 119° for $[Pt_2(H_2PCH_2CH_2PH_2)_2(\mu\text{-}S)_2]$.[49] However, the very bulky 2-diphenylphosphanopyridine (dppy) ligand forces complete planarity in $[Pt_2(dppy)_4(\mu\text{-}S)_2]$.[50] The near planar structure of **5** suggests a substantial steric constraint imparted not only by the phosphine ligand but by the bulky germylene as well. Although the geometry about the Pd and Ge centers is less strained, the steric constraints imparted by the large germylene and phosphine ligands are evident at the S bridges.

Regeneration of Parent Three-Coordinate Pd−Ge Complexes from Bridged Sulfide Complexes. The addition of 5 equiv of free germylene to a benzene-d_6 solution of **2** results in the reformation of the parent complex **1** as monitored by ^{1}H NMR, ^{31}P NMR, and ^{13}C NMR spectroscopy. This transformation occurs slowly in ambient light at room temperature, resulting in 6% conversion to **1** after 2 days. Heating of the solutions to 63 °C speeds up the rate of the conversion to 32%. The greatest degree of conversion occurred under photolytic conditions with 63% of **1** being formed after 48 h of UV exposure. The presence of excess germylene is critical for the regeneration of **1**, as solutions of **2** that did not contain excess germylene showed no reaction under these conditions.

Solutions of **5** to which 5 equiv of germylene was added regenerated **4.** Heating of the solution resulted in 32% conversion to **4** after 48 h. Photolytic conditions were less effective giving 12% conversion to **4** after the same length of time. The presence of excess germylene is necessary to obtain conversion; however, unlike complex **2**, solutions kept in ambient light at room temperature did not react over the time frame of the experiments.

The fate of the S atom in these reactions is not clear. NMR spectra reveal the growth of several other products throughout the course of these reactions. Several new singlets appear in the trimethylsilyl region of the ^{1}H NMR and ^{13}C NMR spectra in addition to the singlet associated with **1** or **4**. This indicates that several new germanium-containing species are formed. It is possible that thiadigermiranes are among these new species as these structures are known to be stable.[51] However, only the reaction of **5** heated with excess germylene showed evidence for the formation of the dimeric germanesulfanone, $\{[(Me_3Si)_2N]_2GeS\}_2$. Both ^{1}H NMR and ^{13}C NMR show a singlet resonances at 0.50 and 7.02 ppm, respectively, consistent with the formation of this dimer. These resonances were not observed in the NMR spectra of any other reactions in this series.

To confirm that the removal of S was dependent on the presence of excess germylene and was not mediated by the formation of phosphine sulfide, solutions containing **2** or **5** and 5 equiv of PEt_3 or PPh_3, respectively, were also examined. With one exception, no reaction occurred in ambient light, heating, or photolytic conditions over the 48 h time course of the experiments. A small amount of phosphine sulfide and **1** (2%) were observed for the reaction of **2** with excess phosphine after 48 h of photolysis.

Formation of $\mathbf{\{(Et_3P)P\overline{d(\mu S)G}e[N(SiMe_3)_2]_2\}_2}$ **(8).** If the reaction of **1** with COS is allowed to stir for several days, a black precipitate deposits, and NMR spectra reveal the growth of several new products in addition to **2**. One of these new products crystallized out of the mixture, and X-ray diffraction revealed a dimeric form of **2**, $\{(Et_3P)P\overline{d(\mu S)G}e[N(SiMe_3)_2]_2\}_2$ (**8**). Each Pd center has lost one phosphine ligand, and the empty coordination site is being filled by coordination to the bridging S atom. The NMR chemical shifts of the germylene trimethylsilyl groups of **8** are coincident with those of **2** at 0.60 ppm, suggesting that the electronic environment around the Ge center is similar. The crystal structure of **8** (Figure 3) reveals that the Pd, Ge, and S atoms form an unusual and almost completely planar arrangement (see Table 2 for relevant dihedral angles). The Pd−Ge bond length of **8** is slightly shorter at 2.3488(3) Å, while the Pd_1−S_{1A} bond length is 2.4645(4) Å, 0.1 Å longer than in **2**. The length of the new bond formed from the bridging S_1 to the Pd_1 center is even longer at 2.5055(5) Å.

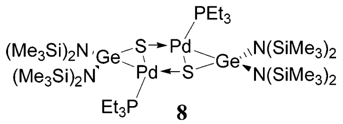

8

The development of a high-yield synthesis for **8** has eluded us. It is not present in reaction mixtures of **1** and COS that have only stirred for several hours. Complex **8** does not appear to form simply from the dimerization of **2**. A THF solution of **2** was allowed to stir for 5 days without any apparent formation of **8**, and benzene solutions of **2** also do

---

(48) Fong, S. W. A.; Hor, T. S. A. *J. Chem. Soc., Dalton Trans.* **1999**, 639−651.

(49) Capdevila, M.; Carrasco, Y.; Clegg, W.; Coxall, R. A.; Gonzalez-Duarte, P.; Lledos, A.; Sola, J.; Ujaque, G. *Chem. Commun.* **1998**, 597−598.

(50) Yam, V. W. W.; Yeung, P. K. Y.; Cheung, K. K. *Chem. Commun.* **1995**.

(51) Tsumuraya, T.; Sato, S.; Ando, W. *Organometallics* **1988**, *7*, 2015−2019.

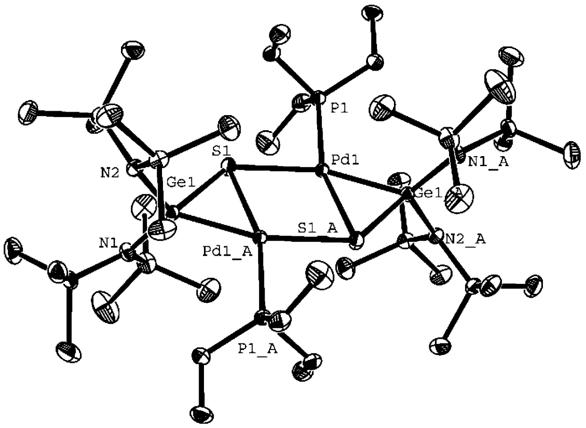

Figure 3. ORTEP representation (50% probability) of $\{(Et_3P)Pd(\mu S)Ge[N(SiMe_3)_2]_2\}_2$ (**8**).

not appear to react on their own, even after heating or photolysis (vide supra). The addition of the phosphine trap, CuCl, or stoichiometric amounts of H_2O or O_2 as phosphine oxidants to solutions of **2** failed to generate **8**. We have also explored the possibility that the CO gas liberated in the reaction may be involved in the formation of the dimer. The addition of CO to solutions of **2**, as well as addition of an equivalent of CO and an equivalent of COS to solutions of **1** or **2**, also failed to generate **8**. Thus far, we have only been able to generate **8** in trace amounts by extending stirring of the reaction that forms **2**. Crystals can be isolated from benzene as part of the purification process for **2**. Although a well-defined method for high-yield isolation of this material has not been developed, we report the structure of this complex here because of its intrinsic novelty and its relationship to the other complexes reported.

Conclusions

We have described new modes of cooperative reactivity for transition metal germylene complexes. Sulfide bridges form via extrusion of the S atom from COS and addition across the Pd−Ge bond without cleavage of the bond. A second sulfide bridge and cleavage of the Pd−Ge bond occurs upon reaction with a second equivalent of COS. The formation of a single or double-bridged sulfide is phosphine dependent. A unique dimeric product is also formed by these reactions. These complexes are the first molecular Pd/Ge/S species to be isolated and characterized, representing a class of complexes that serve as model systems for considering the interactions of S with Pd−Ge heterogeneous catalysts. We have demonstrated the ability of germylene to sequester S in these systems and to regenerate the original Pd^0 metal center, providing insight into potential mechanisms of action of Ge promoters in sulfur resistant catalysis systems.

Acknowledgment. This work was funded by the Research Corporation and the Petroleum Research Fund. Z.T.C. thanks the National Science Foundation for a graduate research fellowship.

Supporting Information Available: X-ray crystallographic data and files in CIF format for **2**, **5**, **7**, and **8**. This material is available free of charge via the Internet at http://pubs.acs.org.

IC034613Z